

# Nonlinear signal transduction network with multistate\*

Han-Yu Jiang, Jun He<sup>†</sup>

School of Physics and Technology, Nanjing Normal University, Nanjing, Jiangsu 210097, China

January 17, 2022

## Abstract

Signal transduction is an important and basic mechanism to cell life activities. The stochastic state transition of receptor induces the release of signaling molecule, which triggers the state transition of other receptors. It constructs a nonlinear signaling network, and leads to robust switchlike properties which are critical to biological function. Network architectures and state transitions of receptor will affect the performance of this biological network. In this work, we perform a study of nonlinear signaling on biological network with multistate by analyzing network dynamics of the  $\text{Ca}^{2+}$  induced  $\text{Ca}^{2+}$  release mechanism, where fast and slow processes are involved and the receptor has four conformational states. Three types of networks, Erdős-Rényi network, Watts-Strogatz network and Barabási-Albert network, are considered with different parameters. The dynamics of the biological networks exhibit different patterns at different time scales. At short time scale, the second open state is essential to reproduce the quasi-bistable regime, which emerges at a critical strength of connection for all three states involved in the fast processes and disappears at another critical point. The pattern at short time scale is not sensitive to the network architecture. At long time scale, only monostable regime is observed, and difference of network architectures affects the results more seriously. Our finding identifies features of nonlinear signaling networks with multistate that may underlie their biological function.

**Keywords:** Signal transduction, Biological network with multistate, CICR, Nonlinear signaling

**PACS:** 87.18.Mp, 87.16.Xa, 87.17.Aa

## 1. Introduction

The signal transduction is important to a variety of intracellular and intercellular processes [1]. The signal propagates between different cellular components and communicates between biological cells. It usually mediates between two receptors by signaling molecule, which changes the conformational state of receptor protein. Generally, the response of receptor is typically a nonlinear function of the local concentration of signaling molecule [2–4]. In this way, signal transduction systems can perform robust switchlike operations [2,5]. The state transition of the receptors triggers or inhibits the release of signaling molecule, which then affects other receptors' state. With such mechanism, the signal propagates on the network of intracellular and intercellular receptors. Given that signal transduction involves a large number of receptors with complex connections by signaling molecule, it is natural to apply the network science to understand their

---

\*Project supported by the National Natural Science Foundation of China (Grants No. 11675228) and China postdoctoral Science Foundation (Grants No. 2015M572662XB).

<sup>†</sup>Corresponding author. E-mail: junhe@njnu.edu.cn

dynamics [6–9]. To keep and regulate the life activity, there exist a variety of signaling networks, such as calcium signaling network, protein-protein interaction networks, and excitation-contraction coupling in muscle tissue [10–12]. Up to now, much efforts have been paid in this direction and some key insights have been achieved using such interdisciplinary approach [13].

In the signal transduction network, the receptors are taken as the nodes which are connected by signaling molecule. Generally speaking, the receptors are not uniformly distributed spatially. Though the connections between the nodes are not directly related to the spatially distribution of receptors, it makes the network architecture more complex. It is also well known that the intracellular space is crowded with organelles and various obstructions [14]. The diffusing signaling molecule has to navigate between complex intracellular structures. Besides, the receptors usually embedded on the biomembrane, which is not flat. For example, the ryanodine receptor (RyR) distributes on the endoplasmic reticulum, which is folded in the cytoplasm, and some parts of different sheets may be very close to each other. The calcium signal transduction also happens at the ER-PM junction [15–17]. In this way, signals can be communicated between distant regions in the biomembrane. The connections between receptors can be very complex. In the words of the network science, the single transduction should be on some types of the networks. However, based on the current knowledge, we do not know their explicit network architectures. Thus, it is interesting to study the effect of different network architectures on signal transduction, especially whether the biological function performs stably and similarly with different network architectures.

The bistable regime can emerge from the network dynamics in a study of the propagation of nonlinear singling on the network [4] as in electronic systems [3] where the network architecture was not considered. In their work, only two states, a closed state and an open state, were considered for a receptor [4]. In many signaling system, the receptor has more conformational states, the transition between these states may exhibit more complex patten of the signaling transduction. The  $\text{Ca}^{2+}$  induced  $\text{Ca}^{2+}$  release mechanism (CICR) is a basic mechanism of the calcium transduction system, which is important second messenger in the biological system, and widely involves in the regulation of cell life activities, including cell membrane permeability, cell secretion, metabolism and differentiation [18,19]. In the literature [20], a simplified mechanism that mimics "adaptation" of the RyR has been developed to reproduce experimental data from cardiac cells. In such model, the nodes of the calcium signaling network, RyRs, have four states. Moreover, among the transitions between these states, there are two fast processes and one slow process. In this study, we will study the CICR on the network to explore the behavior of signaling networks with multistate in which nodes are regulated by reaction rates nonlinearly. Our main finding is that the second open state in CICR is essential to produce the bistable regime, and the inclusion of the slow process makes the dynamics of the calcium singling network exhibit different patterns at different time scales. The results may underlie the biological function of the CICR and be helpful for understanding other networks with multistate.

## 2. Mechanism of CICR

In the current work, we take an RyR, the receptor of the CICR mechanism as a node of network. RyR has four states as shown in Fig. 1. States  $C_1$  and  $C_2$  are closed states, in which no calcium will be released, and states  $O_1$  and  $O_2$  are open states, in which RyR releases calcium. The transitions between different states of an RyR in an environment with concentration  $[\text{Ca}^{2+}]$  are also illustrated in Fig. 1. The relevant parameters have been extracted from the experiment, and listed in Table 1.

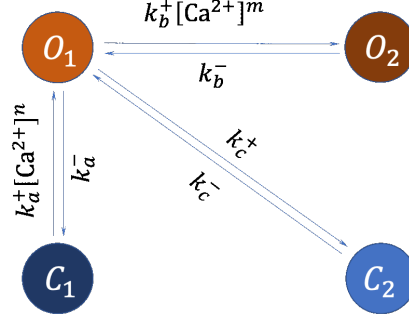


Figure 1: Schematic diagram of transitions among the four states of the RyR [20].

Table 1: RyR kinetic constants [20]. The parameters  $n$  and  $m$  were also determined as 4 and 3, respectively.

rate	$k_a^+$	$k_a^-$	$k_b^+$	$k_b^-$	$k_c^+$	$k_c^-$
Value	1500	28.8	1500	385.9	1.75	0.1
Unit	$\mu\text{M}^{-4}\text{s}^{-1}$	$\text{s}^{-1}$	$\mu\text{M}^{-3}\text{s}^{-1}$	$\text{s}^{-1}$	$\text{s}^{-1}$	$\text{s}^{-1}$

The state  $C_1$  is dominant at a low concentration  $[\text{Ca}^{2+}]$ , for example  $0.1 \mu\text{M}$ . If the  $[\text{Ca}^{2+}]$  increases, the RyR will be activated from the closed state  $C_1$  to an open state  $O_1$  at a rate of  $k_a^+[\text{Ca}^{2+}]^n$ , and deactivates back to  $C_1$  state at a rate of  $k_a^-$ . The open state  $O_1$  also may be activated to the second open state  $O_2$  at a rate of  $k_b^+[\text{Ca}]^m$  and back to the first open state  $O_1$  at a rate of  $k_b^-$ . Such process is important to keep the plateau open probability as suggested in Ref. [20]. It is also important to obtain the bistable regime in the current work. The transition between first open state  $O_1$  and the second closed state  $C_2$  is independent on the concentration  $[\text{Ca}^{2+}]$ . And compared with the rates of processes  $C_1 \rightleftharpoons O_1$  and  $O_1 \rightleftharpoons O_2$ , the process  $O_1 \rightleftharpoons C_2$  should be slow, which makes the decrease of the fractions of open states be a long-time-scale process.

With the above mechanism, we study the dynamics of the CICR on the network. For a network with  $N$  nodes, the state of a node can be denoted as vectors,  $[1, 0, 0, 0]$ ,  $[0, 1, 0, 0]$ ,  $[0, 0, 1, 0]$ ,  $[0, 0, 0, 1]$  for  $C_1$ ,  $O_1$ ,  $C_2$  and  $O_2$ , respectively. The overall state of the network can be written as a  $4 \times N$  matrix  $S(t)$ , which revolves with time  $t$ . Besides the nodes, i.e., RyR, we need connections between them to study the dynamics of the CICR network. As in Ref. [4], we assume the concentration  $[\text{Ca}^{2+}]$  at an RyR is determined by a general background concentration  $c_0$  and calcium released by other RyRs. Hence, it can be obtained by the states of other nodes as

$$[\text{Ca}^{2+}](t) = c_0 + r \sum_{m,j}^N A_{ij} S_{mj}(t), \quad (1)$$

where  $m = 1, 2, 3, 4$  corresponds to states  $C_1$ ,  $O_1$ ,  $C_2$  and  $O_2$ , respectively, and  $i$  or  $j$  are the number of the nodes. It is nature to assume a small general background concentration  $c_0$ ,  $0.1 \mu\text{M}$ , in this work, and the concentration is mainly from the calcium released from other nodes. Hence, only the nodes in two open states contribute to the concentration, which is denoted as  $S_{2j}$  and  $S_{4j}$ . The  $A_{ij}$  denotes adjacency matrix, which is different for different types of networks. The parameter  $r$  gives the strength of connection between two nodes, which is assumed as a general constant. A more appropriate parameter can be defined as  $s = r\langle k \rangle / c_0$  with the average degree  $\langle k \rangle = 1/N \sum_i^N k_i$  and  $k_i = \sum_i^N A_{ij}$ , which will be adopted in the following calculation (its meaning can be seen more clearly under the mean-field ansatz in section 4.).

### 3. Dynamics of CICR on the network

In this section, we will consider the dynamics of CICR on the network. In our study, we will perform the investigation with three different types of networks, Erdős-Rényi (ER) network, Watts-Strogatz (WS) network and Barabási-Albert (BA) network. The networks are generated with the help of the NetworkX package in Python Language. In the ER network, the two nodes are connected with a fixed probability  $p$ . In the WS network, every node connects to  $k$  neighbor nodes, and two nodes are connected with fixed probability  $p$ . Such network may be more appropriate to describe the behavior of the CICR mechanism because usually the calcium released by a RyR will induce the release of neighbor RyRs on the endoplasmic reticulum while some other distant RyRs may be also activated due to the folding of the membrane. We also consider the BA network, which is formed by adding a sequence of  $m$  new nodes to an existing network. By the generated network, we have the network adjacency matrix  $A$  in Eq. 1.

With overall state matrix  $S$ , it is easy to characterize the activity of the network by computing the fraction of node which is in an state  $i$  at time  $t$  as

$$p_i(t) = \frac{1}{N} \sum_{j=1}^N S_{ij}(t). \quad (2)$$

To study the dynamics, we also should consider an ensemble of initial conditions where activity level of network is varied. We choose initial conditions that the node  $i$  has a probability  $h$  at  $C_1$  and  $1 - h$  at  $O_1$ . For simplicity, we do not consider other possible initial conditions with  $O_2$  and  $C_2$  states, which should provide similar conclusion. Here we simulate initial conditions where  $h = i/(K - 1)$  and  $i = 0, 1, \dots, K - 1$ . With such treatment, we can explore the time revolution of a range of random initial conditions  $S^i(0)$ .

With the network adjacency matrix  $A$  and the initial state matrix  $S^i(0)$  obtained as above, we can simulate the time revolution of the dynamics of the CICR on the network under the mechanism in Fig. 1. In the simulation, we adopt network with  $N = 500$  nodes, and choose  $K = 6$  random initial conditions. We consider the time revolutions of the fractions of four states on three networks considered. The parameters are chosen as  $p = 0.1$  for ER network,  $k = 5$  and  $p = 0.1$  for WS network, and  $m = 10$  for BA network. Since we need synchronize the time for all nodes in the network to give the explicit time revolution of fractions of four states of node, the Gillespie algorithm is not practical and simulation with fixed time step is performed to simulate the transitions between the four states of the RyR in the current work.

In Ref. [4], the nonlinear network with a closed and an open state exhibits bistable regime with a small  $\eta$  in their work. If we only consider  $C_1$  and  $O_1$  state, an explicit calculation suggests that there are no bistable regime emerging because the values of rates  $k_a^+$  and  $k_a^-$  shown in Table 1, which were extracted from experimental data leads to a large  $\eta$ . It is interesting to see that the bistable regime recovers after state  $O_2$  is added. However, the inclusion of the slow process  $O_1 \rightleftharpoons C_2$  will break such bistable regime, which can be seen in the results at different strengths of connection  $s$  illustrated in Figs. 2-5.

In Fig. 2, the results with small strength of connection  $s = 1$  are presented. We provide the results at both short time and long time scales to show the effects of fast processes and slow process. The results at medium time scale are also given as a reference of general picture of the time revolution. The time revolution of the fractions of four states on three networks exhibit very similar behaviors. The open state  $O_1$  will deactivate rapidly within a relaxation time  $\tau \sim 0.1$  s (see Fig. 2a1, b1, and c1). At such time scale, the state  $O_2$  is nearly not activated, and the fraction of state  $C_2$  increases very slowly. Such pattern keeps up to a time about 1 s (see Fig. 2a2, b2, and c2). At the scale of 10 s, the slow process takes effect. The fractions of states  $C_2$  and  $C_1$  decrease and increase a little, respectively, and approach to steady states (see

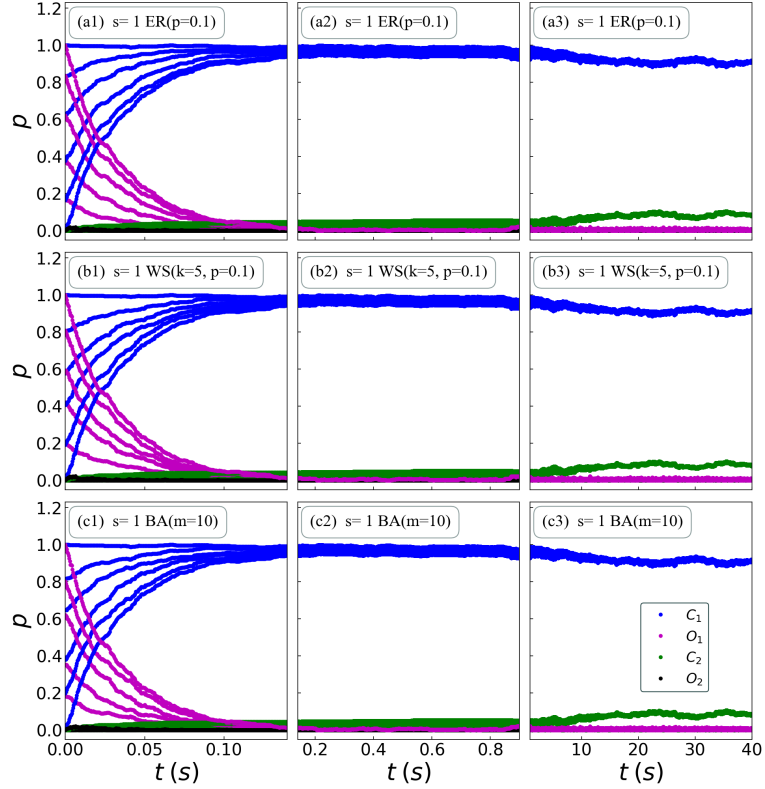


Figure 2: The fractions of states  $C_1$  (blue dot),  $O_1$  (magenta dot),  $C_2$  (green dot) and  $O_2$  (dark dot) on three networks as a function of time for an ensemble of initial conditions with strength of connection  $s = 1$ . The panels (a1, a2, a3) are for the ER networks with  $p = 0.1$  at short, medium, and long time scales, respectively. The panels (b1, b2, b3) are for the WS networks with  $K = 5$  and  $p = 0.1$ , and the panels (c1, c2, c3) for the BA networks with  $m = 10$ . In the calculation, 100000 time steps are adopted.

Fig. 2a3, b3, and c3).

In Fig. 3, the results with  $s = 5$  are presented. Compared with the results with strength  $s = 1$ , the behaviors of the activity of the network become more complex. At short time scale, the state  $O_1$  does not deactivate completely at  $t \sim 0.1$  s. With the time revolution, the fraction of state  $O_1$  will approach to zero finally as shown in the mediate panels. In fact, if we neglect the slow process, the activity of the network will enter a bistable regime at long time scale. However, the effect of the slow process  $O_1 \rightleftharpoons C_2$  makes the time not enough to exhibit such behavior, which will be discussed later. At long time scale, the tendencies of fractions of states  $O_1$ ,  $C_1$ , and  $O_2$  at short time scale are smeared. A stable pattern as in the case with  $s = 1$  emerges at time  $t > 20$  s. Besides, with strength  $s = 5$ , three networks also exhibit analogous behaviors.

In Fig. 4, the results with  $s = 10$  are presented. In this case, the quasibistable regime becomes more clearly. At short time scale, the quasi-steady states can be seen clearly (here and hereafter, we will call the approximate steady state and approximate bistable regime at short time scale as “quasi-steady state” and “quasi-bistable regime” to distinguish them from the real steady state at long time scale and bistable regime only with fast processes). With the increase of the strength of connection  $s$ , the relaxation time of the fast process becomes smaller, about 0.01 s with connection  $s = 5$ . However, as shown in Fig. 1, the slow process is independent of the  $s$ , which is the reason why the quasi-steady states here are more obvious than those with small strength. One can observe the transitions from a quasi-steady state to another quasi-steady

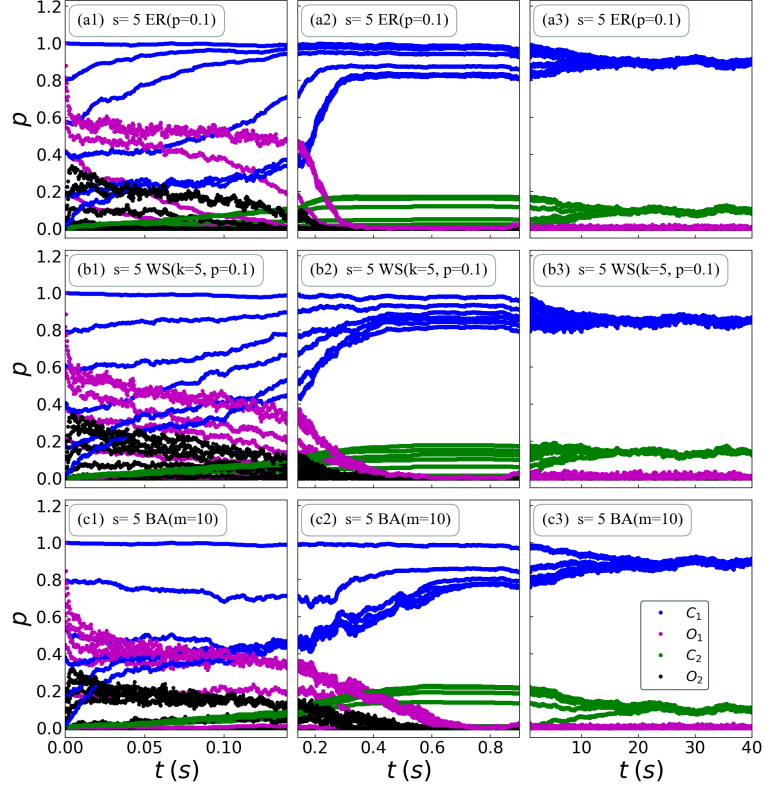


Figure 3: The fractions of four states. The same as Fig. 2, but with strength of connection  $s = 5$ .

state. For example, on WS network, the state  $O_1$  has two quasi-steady states, one is about 0 and the other about 0.2. At a time about 0.05 s, the network leaves the former and jumps to the latter. The state  $O_2$  also may jump from a state about 0 to the state about 0.8. The values of the quasi-steady states for ER and WS networks are almost the same. However, the BA network has a larger fraction for state  $O_2$ . At a time scale of 0.1 s, the fraction of state  $O_2$  decreases until reaching zero.

The decrease of fraction of state  $O_2$  can be seen at time scale of 1 s. The fraction of state  $C_2$  increases first, but at long time scale its behaviors are different for different networks. On ER network, the fraction of state  $C_2$  tends toward a stable value about 0.1 and the one of state  $C_1$  toward a value about 0.9. The nodes of the network are almost occupied by these two states at long time scale, the fractions of states  $O_1$  and  $O_2$  are about zero. On WS network, the stable value for state  $C_2$  is about 0.5, higher than the one for state  $C_1$ , about 0.4. Besides, the system approaches steady states at time smaller than 10 s, which is different from the pattern on the ER network. For BA network, the tendencies of fractions of four states are analogous to the case on ER network. However, the statistical transitions between the two steady states and state  $O_1$  by fast processes make the situation more complicated because states  $C_1$  and  $C_2$  connected by  $O_1$ , which is usually very low at long time scale.

Now, we turn to a large strength of connection  $s = 45$ , and the results are presented in Fig. 5. At short time scale, one can find that after a very small relaxation time, the states of the network concentrates to the state  $O_2$ . The quasi-bistable regime in previous figures disappears in the large strength. With time revolution, the fraction of state  $O_2$  decreases, and reaches a value about 0.2 or smaller at larger time scale. The state  $C_2$  becomes dominant. The fraction of state  $O_1$  keeps a low level at all time scales, while the state  $C_1$  is observable on WS scale at long time scale.

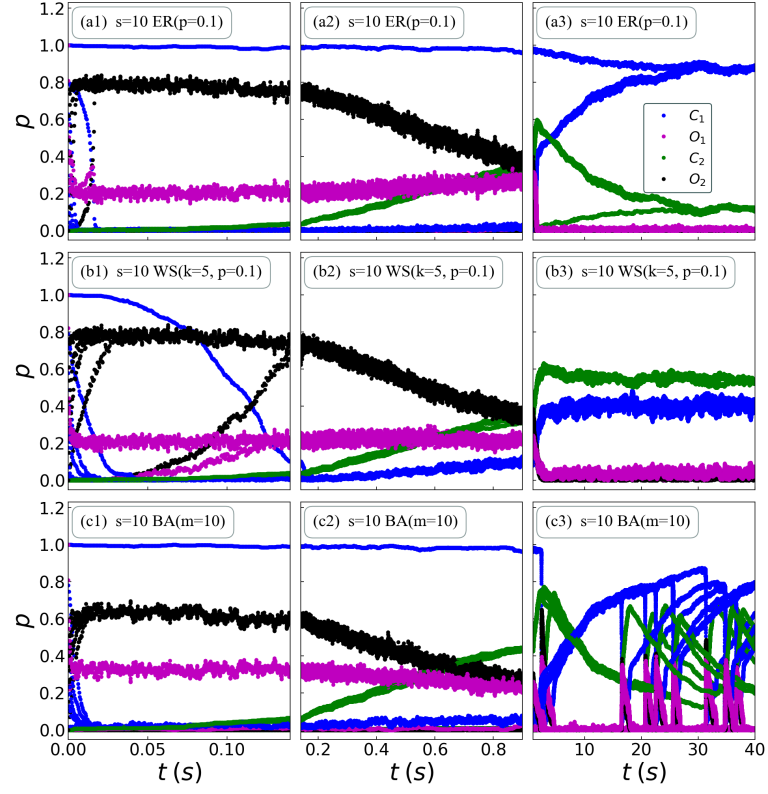


Figure 4: The fractions of four states. The same as Fig. 2, but with strength of connection  $s = 10$ .

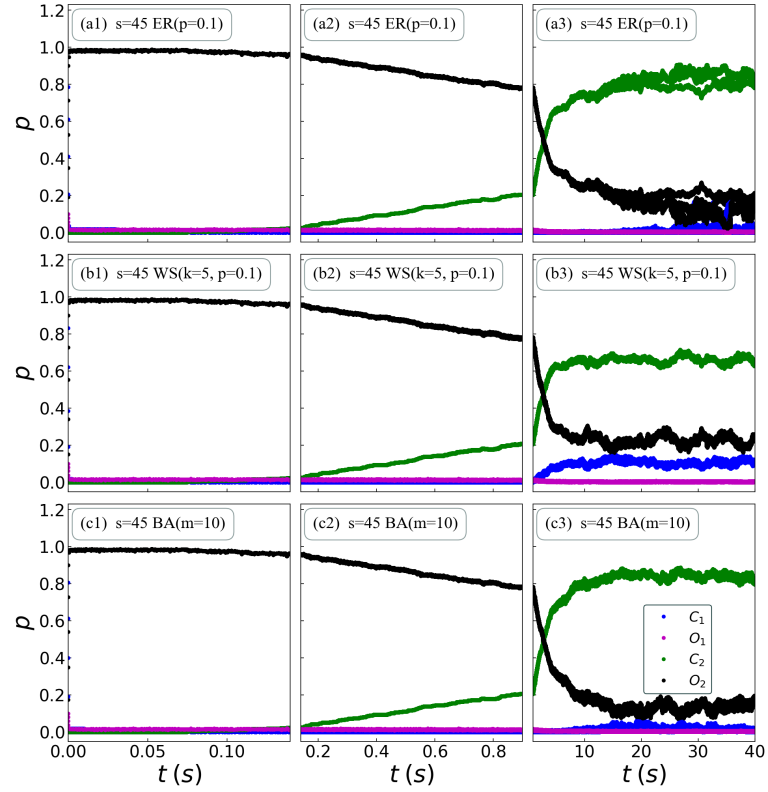


Figure 5: The fractions of four states. The same as Fig. 2, but with strength of connection  $s = 45$ .



## 4. Pattern of steady states on network

In the above, we present the time revolution of the fractions of four states on three networks. One can find that at small strength of connection  $s$ , the network is nearly not activated. With increasing of the strength of connection, quasi-bistable regime emerges at short time scale, where the fast processes play the dominant role. However, the low process breaks the quasi-steady states with the time revolution, and network revolves to the steady states at long time scale. And with a very large strength of the connection, the quasi-bistable regime disappears. Since the steady states are more interesting in biological function. In this section, we will discuss the dependence of the quasi-steady states on networks.

To understand the basic feature of the network dynamics, we first provide the mean field (MF) ansatz of the system considering homogeneous [4]. Under this ansatz, we assume all nodes revolve with time in the same manner, which leads to the state function  $S_{ij} = S_{i0}$  with  $i$  and  $j$  denoting the four states and  $N$  nodes, respectively. Hence the calcium concentration can be written as

$$[\text{Ca}^{2+}] = c_0 + sc_0(p_{O_1} + p_{O_2}). \quad (3)$$

Here we apply  $\langle k \rangle = \sum_j A_{ij}$  and  $S_{20} = p_{O_1}$  and  $S_{40} = p_{O_2}$  under MF ansatz. Here and hereafter, for fractions of the states, we use  $C_1$ ,  $O_1$ ,  $C_2$  and  $O_2$  instead of 1, 2, 3, and 4 for convenience to understand. The dynamics equation can be written as,

$$\frac{dp_{C_1}}{dt} = -k_a^+[c_0 + sc_0(p_{O_1} + p_{O_2})]^4 p_{C_1} + k_a^- p_{O_1}, \quad (4)$$

$$\begin{aligned} \frac{dp_{O_1}}{dt} &= k_a^+[c_0 + sc_0(p_{O_1} + p_{O_2})]^4 p_{C_1} - k_a^- p_{O_1} \\ &\quad - k_b^+[c_0 + sc_0(p_{O_1} + p_{O_2})]^3 p_{O_1} \\ &\quad + k_b^- p_{O_2} - k_c^+ p_{O_1} + k_c^- p_{C_2}, \end{aligned} \quad (5)$$

$$\frac{dp_{O_2}}{dt} = k_b^+[c_0 + sc_0(p_{O_1} + p_{O_2})]^3 p_{O_1} - k_b^- p_{O_2}, \quad (6)$$

$$\frac{dp_{C_2}}{dt} = k_c^+ p_{O_1} - k_c^- p_{C_2}, \quad (7)$$

with  $p_{C_1} + p_{O_1} + p_{C_2} + p_{O_2} = 1$ .

Based on the parameters in Table 1, the processes in Eqs. (4, 6) are fast processes while the last one is slow process. If we consider all three processes, we will reach the steady states at long time scale. Hence, first, we consider the case with the last process  $O_1 \leftrightarrow C_2$  turning off. With such treatment we can obtain steady states at a long time scale which correspond to results of full model at short time scale. The steady states corresponds to the stationary points, which satisfy the algebraic condition as

$$\begin{aligned} 0 &= -k_a^+[c_0 + sc_0(p_{O_1} + p_{O_2})]^4 p_{C_1} + k_a^- p_{O_1}, \\ 0 &= k_b^+[c_0 + sc_0(p_{O_1} + p_{O_2})]^3 p_{O_1} - k_b^- p_{O_2}, \end{aligned} \quad (8)$$

where  $p_{C_1} + p_{O_1} + p_{O_2} = 1$ , and we still use a low background  $c_0 = 0.1 \mu\text{M}$  and consider the variation of the parameter  $s$ , which reflects the strength of the connections between nodes on the network.

In Fig. 6, we present the steady states obtained with above conditions. Under the MF ansatz, the difference of networks is smeared, and the effect of network is absorbed into the strength parameter  $s$ . For the results with low strength, the network can not be activated as in Fig. 2, which leads to a meaningless steady state with  $C_1 = 1$ . With the strengthening of the connection between nodes, a bistable regime of fraction of state  $C_1$  emerges at  $s \sim 5$ . Besides the steady state at



$C_1 \sim 0$ , there exists another steady state at about 0.2, which decrease rapidly with the increase of the strength  $s$ . The steady state at about 1 for state  $C_1$  keeps until an  $s$  about 20, and disappears there. For state  $O_1$ , there exists a steady state at small  $s$ , and a new steady state about 0.5 appears at  $s$  about 5 and decreases to zero slower than state  $C_1$ . At an  $s$  about 20, the steady state about 0 for state  $O_1$  disappears and only one steady state keeps. The state  $O_2$  also exhibits bistable regime with a steady state about 0.5 and a steady state about 0. The higher one will increase to about 1 with the increase of  $s$ , and the steady state about 0 disappear at  $s$  about 20 also. Hence, under MF ansatz, for all three states (the  $C_2$  state is removed here), the fractions of states are monostable at  $s \lesssim 5$ , bistable at  $20 \gtrsim s \gtrsim 5$ , and monostable again in  $s \gtrsim 20$ .

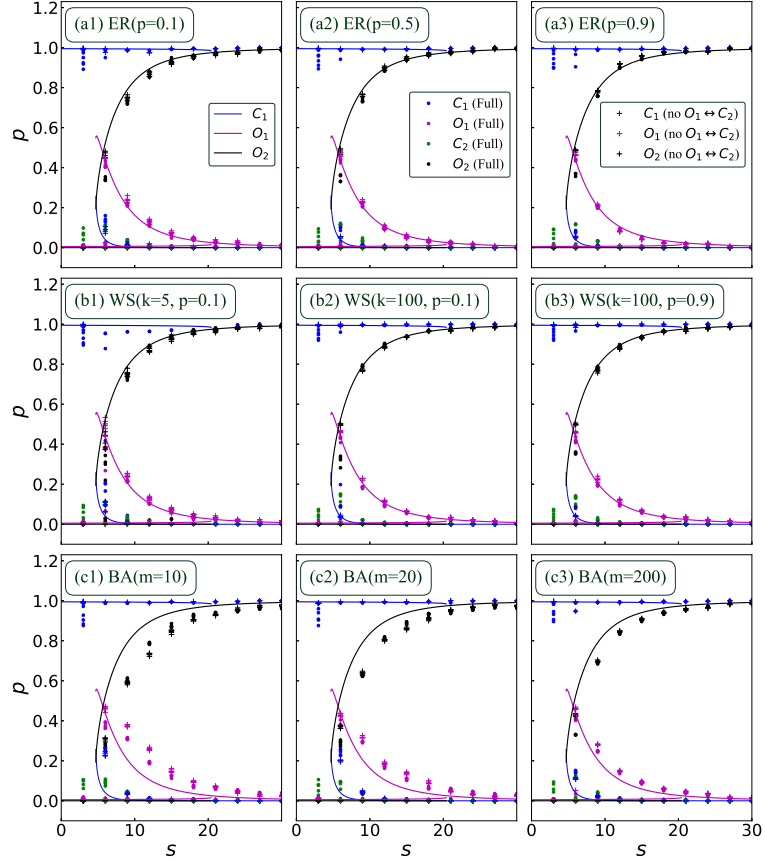


Figure 6: The steady states on networks with different parameters with the variation of the strength of connection  $s$ . The lines are for the MF ansatz with the process  $O_1 \leftrightarrow C_2$  turning off (Eq. 8). The symbols “.” and “+” are for the results at small time scale with full model, and results after turning off the  $O_1 \leftrightarrow C_2$  process, respectively.

For the realistic networks, we still consider the three networks in previous calculation with more parameters. With the  $O_1 \leftrightarrow C_2$  process turning off, the steady states can be reached at time long enough. As shown in Fig. 6, one can find that the model only with fast processes produce a result (symbol “+”), which fit the curves under MF ansatz very well on the ER and WS networks. The result on BA network deviates from the MF results a little larger. Besides, the results with different parameters of each network are similar to each other. We also provide the results with full model (symbol “.”). Because the pattern of the steady states will be broken by the slow process, we choose time points  $t = 0.4 \times 0.1^s$  to extract the values of fractions where the quasi-steady states can be seen obviously but the effect of the slow process is still very small. It can be found that the quasi-steady states are close to these only with the fast processes at most values of  $s$ , except about 6. As shown in Fig. 3, with a strength about 6, the effect of the slow process becomes obvious within the relaxation

time of the quasi-steady states. Generally speaking, the simulation results are close to these under MF ansatz.

Now, we consider the cases with slow process, the stationary points should satisfy the algebraic conditions as

$$\begin{aligned} 0 &= -k_a^+[c_0 + sc_0(p_{O_1} + p_{O_2})]^4 p_{C_1} + k_a^- p_{O_1}, \\ 0 &= k_b^+[c_0 + sc_0(p_{O_1} + p_{O_2})]^3 p_{O_1} - k_b^- p_{O_2}, \\ 0 &= k_c^+ p_{O_1} - k_c^- p_{C_2}, \end{aligned} \quad (9)$$

with  $p_{C_1} + p_{O_1} + p_{C_2} + p_{O_2} = 1$ .

In Fig. 7, we present the steady states obtained from the above conditions. At first sight, one can find that after including the slow process, the pattern of steady states changes completely. It is also the reason of the different pattern for time revolution at short and long time scales shown in Figs. 2-5. For the  $s$  from 0 to about 50, no bistable regime emerges for all four states on three networks. The MF results suggests that with weak connection, small  $s$ , the fraction of state  $C_1$  is about 1 and will decreases rapidly at about 30, and to a very small value at about 50. The fraction of state  $C_2$  exhibits almost reverse behavior, about 0.1 at  $s$  about 0, and increases fast at  $s$  about 30, and up to about 0.8 at  $s$  about 50. The network is dominant by these two closed state, which satisfy the requirement of the biological function.

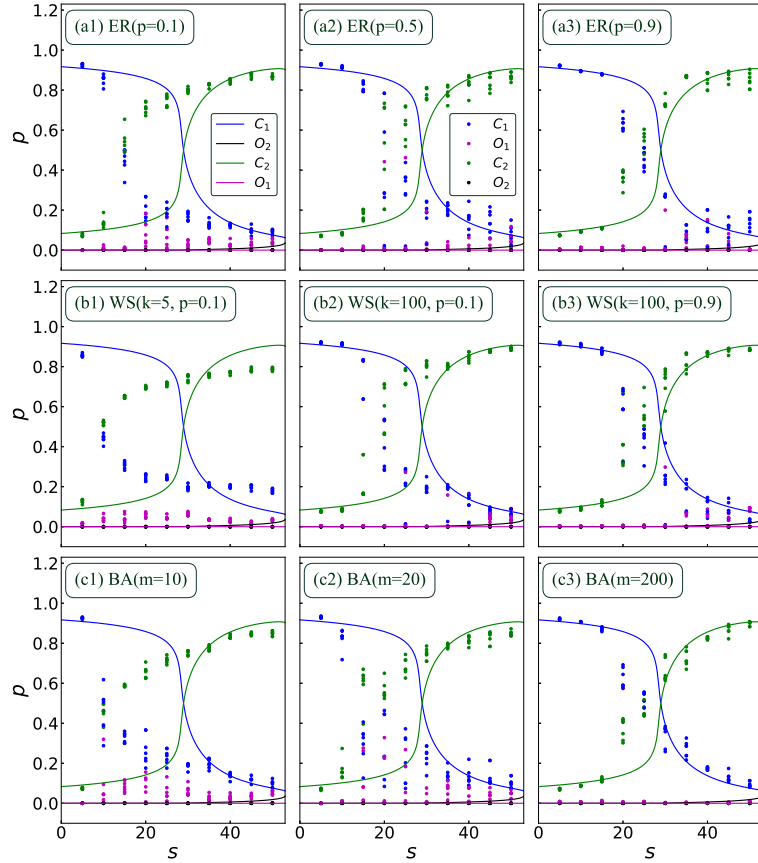


Figure 7: The steady states on networks with different parameters with the variation of the strength of connection  $s$ . The lines are for the MF ansatz of full model (Eq. 9) and the symbols “.” is for the results of the simulation of full model at long time scale.

The simulation results of the full model are also presented in the Fig. 7. Different from results at short time scale, the results for different networks and parameters are different, and deviate from MF results obviously. For ER network, the

cross point of  $C_1$  and  $C_2$  is lower than MF curves. With the increase of  $p$ , the simulation results become closer to the MF results. Such situations can be found also for WS and BA networks.

## 5. Discussion and summary

Signal transduction is an important mechanism in living things to regulate cell life activities. The signal usually mediates from a receptor to another receptor by releasing singling molecular which can change the states of the receptor. It suggests that the signal propagates on a biological network with receptors as nodes. Hence, to study the mechanism of the signal transduction, we need consider the network architecture.

The signal transduction on the network may exhibit different behaviors from these without considering the network architecture. In Ref. [4], the authors studied the dynamics of a two-state transition model on networks. The bistable regime was observed in their calculation. However, if we apply their model to the important CICR mechanism in the calcium signaling transduction, the two-state transition model, states  $C_1$  and  $C_2$  in the current work, does not produce any bistable regime in our calculation. It is interesting to see that the bistable regime is reproduced if we include second open state  $O_2$  to states  $C_1$  and  $O_1$ . Such results suggest that the network with more states provides more biological patterns than in the two-states model.

In the CICR mechanism, the transitions between states  $C_1$ ,  $O_1$  and  $O_2$  are all fast processes. The inclusion of state  $C_2$  introduces a slow process, with which the network deactivates with time revolution. The dynamics of the CICR exhibits different patterns at different time scales. Though with this slow process the system tends to closed states in any case, with different strengths of the connection the system tends to different closed states. Weak connection between nodes leads to a large fraction of  $C_1$  state while strong connection to a large fraction of  $C_2$  state.

In this study we consider three types of networks, Erdős-Rényi network, Watts-Strogatz network and Barabási-Albert network, with different parameters. The pattern at short time scale is not sensitive to the network architecture, and close to MF results. At long time scale, only monostable regime is observed. The difference of network architectures affects the results more seriously, and deviates from the MF results at most cases.

In summary, our study shows that nonlinear network with multistate exhibits rich patterns, especially after the processes with different time scales are included. The second open state of CICR is found essential to reproduce the bistable regime at short time scale. Our finding identifies features of biological signaling networks that may underlie their biological function. The results are also helpful to understand other networks with multistate.

## References

- [1] Kalckar H 1991 *Annu. Rev. Biochem.* **60** 1-37
- [2] Fang X, Kruse K, Lu T, and Wang J 2019 *Rev. Mod. Phys.* **91** 045004
- [3] Braichenko S, Bhaskar A, and Dasmahapatra S 2018 *Phys. Rev. E* **98** 032413
- [4] Hernandez-Hernandez G, Myers J, Alvarez-Lacalle E, and Shiferaw Y 2017 *Phys. Rev. E* **95** 032313
- [5] Kholodenko B 2006 *Nat. Rev. Mol. Cell. Biol.* **7** 165
- [6] Barabási A, Oltvai Z 2004 *Nat. Rev. Genet.* **5** 101

- [7] Tong A H Y, Lesage G, Bader G D, Ding H, Xu H 2004 *Science* **303** 808
- [8] Albert R 2005 *J Cell. Sci.* **118** 4947
- [9] Barabási A 2016 *Network science* (Cambridge: Cambridge University Press)
- [10] Li F, Long T, Lu Y, Ouyang Q, Tang C 2004 *Proc. Nat. Acad. Sci.* **101** 4781
- [11] Bers D 2000 *Nature* **415** 198
- [12] Berridge M, Bootman M, and Lipp P 1998 *Nature* **395** 645
- [13] Gosak M, Markovič R, Dolenšek J, Rupnik M, Marhl M, Stožer, M. Perc A 2018 *Physics of Life Reviews* **24**, 118
- [14] Rothman J 1994 *Nature* **372** 55
- [15] Jing J, He L, Sun A, et al. 2015 *Nature Cell Biology* **17** 1339
- [16] Prakriya M, Lewis R 2015 *Physiological Reviews* **95** 1383
- [17] Jiang H Y, He J 2021 *Commun. Theor. Phys.* **73** 015601.
- [18] Clapham D 2017 *Cell* **131** 1047
- [19] Berridge M 2016 *Physiol. Rev.* **96** 1261
- [20] Keizer J, Levine L 1996 *Biophysical Journal* **71** 3477